16th European Signal Processing Conference (EUSIPCO 2008), Lausanne, Switzerland, August 25-29, 2008, copyright by EURASIP

SUBSPACE INTERSECTION METHOD OF BEARING ESTIMATION IN SHALLOW OCEAN USING ACOUSTIC VECTOR SENSORS

K.G. Nagananda and G.V. Anand

Department of Electrical Communication Engineering
Indian Institute of Science, Bangalore 560012, INDIA
Phone: +91-80-22932277. Fax: +91-80-23600563
E-mail: kgnagananda@ece.iisc.ernet.in, anandgv@ece.iisc.ernet.in
Web: http://www.ece.iisc.ernet.in

ABSTRACT

The subspace intersection method (SIM) provides asymptotically unbiased bearing estimates of multiple acoustic sources in a range-independent shallow ocean using a one-dimensional search without prior knowledge of source ranges and depths. The original formulation of this method is based on deployment of a horizontal linear array of hydrophones which measure acoustic pressure. In this paper, we extend SIM to an array of vector sensors which measure acoustic pressure as well as all components of particle velocity. Use of vector sensors reduces the minimum number of sensors required by a factor of 4, and also eliminates the constraint that the intersensor spacing should not exceed half wavelength. The performance enhancement due to the additional information provided by the vector sensors is illustrated through simulation results.

1. INTRODUCTION

High-resolution bearing estimation or direction-of-arrival (DOA) estimation is one of the important steps in localization of acoustic sources in the ocean. Several methods have been used to solve this problem with MUSIC [1] and ESPRIT [2] algorithms being the prominent ones. These algorithms, however, assume plane-wave propagation leading to biased bearing estimates due to the multimode nature of acoustic propagation in the ocean. The bias increases with increasing number of propagating modes in the ocean. Matched field processing (MFP) techniques [3] overcome this problem at the expense of computational complexity, since MFP replaces the one-dimensional search of the above mentioned methods by a three-dimensional search in the bearing-range-depth space. The subspace intersection method (SIM) presented in [4] attempts to alleviate the problem of both bias and computational complexity. Bias is eliminated by replacing the invalid plane-wave propagation model by a more appropriate normal mode propagation model. SIM involves a one-dimensional search without any prior knowledge of the range and depth, thereby decreasing the computational complexity.

The above-mentioned methods make use of the conventional scalar sensors which measure only the acoustic pressure. Nehorai and Paldi [5] presented a method of source localization using an array of acoustic vector sensors (AVS), which can simultaneously measure acoustic pressure and the three Cartesian components of particle velocity at a point. The additional information provided by an AVS can be utilized for better localization. But most AVS array processing techniques including [5] consider a plane wave acoustic propagation model which is not valid for shallow ocean. A maximum likelihood estimation method, which was proposed recently [6], uses a valid model of shallow ocean acoustic propagation. But this method does not have the high resolution capability of SIM, and also it is highly computation intensive.

In this paper we attempt to unify the two frameworks - subspace intersection method and vector sensors, for high-resolution bearing estimation of multiple sources in shallow ocean. No assumption is made on the prior knowledge of source ranges and depths. We compare the performance of SIM with vector and scalar sensor arrays, and show that the use of vector sensors leads to a reduction in the number of sensors, lower rms estimation errors, elimination of spacing constraints, and improved localization performance in the end-fire direction.

The outline of the paper is as follows. In Section 2, we present the AVS array data model for a horizontally stratified ocean. The structure of the noise covariance matrix and a whitening transformation are discussed in Section 3. The subspace intersection method for a vector sensor array is presented in Section 4. Simulation results are presented in Section 5. Section 6 concludes the paper.

2. AVS ARRAY DATA MODEL

The shallow ocean is modeled as a horizontally stratified water layer of constant depth h overlying a horizontally stratified fluid bottom. The variation of its acoustic properties in the horizontal direction is assumed to be negligible in the range of interest. Consider J mutually uncorrelated narrowband point sources of center frequency $\omega/2\pi$ located at depths z_j and ranges r_j with respect to the reference sensor (first sensor) of a horizontal linear array of acoustic vector sensors, also known as vector hydrophones. Source azimuth angles $\phi_j (j = 1,...J)$ are measured with respect to the axis of the array. The array has M equispaced sensors at a spacing of d meters, all lying at a depth of z meters below the ocean surface. Assuming the sensor array to be in the far field region with respect to all sources, the expressions for pressure and particle velocity at the m^{th} sensor due to the j^{th} source are given by [6, 7]

$$p_{mj} = \sum_{n=1}^{N} b_{nj} e^{i[(m-1)k_n d cos\phi_j - \omega t]}, \tag{1}$$

$$v_{xmj} = \frac{cos\phi_j}{\omega\rho} \sum_{n=1}^{N} k_n b_{nj} e^{i[(m-1)k_n d cos\phi_j - \omega t]}, \tag{2}$$

$$v_{ymj} = \frac{sin\phi_j}{\omega\rho} \sum_{n=1}^{N} k_n b_{nj} e^{i[(m-1)k_n d cos\phi_j - \omega t]}, \tag{3}$$

$$v_{zmj} = \frac{1}{\omega\rho} \sum_{n=1}^{N} \left[\frac{-i\psi_n^{'}(z)}{\psi_n(z)} \right] b_{nj} e^{i[(m-1)k_n d cos\phi_j - \omega t]}, \tag{4}$$

where

$$b_{nj} = \frac{2\sqrt{2\pi} e^{i\pi/4}}{h} \psi_n(z) \psi_n(z_j) \left[\frac{e^{-\delta_n r_j} e^{ik_n r_j}}{\sqrt{k_n r_j}} \right] s_j(t), \tag{5}$$

N is the number of normal modes in the oceanic waveguide, $[\delta_n; n = 1,...,N]$ are the attenuation co-efficients,

$[\psi_n(z);\ n=1,...,N]$ are the eigenfunctions and $[k_n;\ n=1,...,N]$ are the eigenvalues obtained by solving the Sturm-Liouville type characteristic differential equation (with appropriate boundary conditions at $z=0$ and $z=h$):

$$\frac{d^2\psi_n(z)}{dz^2}+\left[k^2(z)-k_n^2\right]\psi_n(z)=0,$$

$k(z)=\omega/c(z)$, h is the depth of the water layer, $c(z)$ is the sound speed in water at depth z, $c_b(z)$ is the sound speed in bottom at depth z, $\rho(z)$ and $\rho_b(z)$ are the densities of water and ocean bottom, respectively, at depth z, p_{mj} is the acoustic pressure at the m^{th} sensor due to the j^{th} source, $\left(v_{xmj},v_{ymj},v_{zmj}\right)$ are the x, y and z-components respectively of the particle velocity at the m^{th} sensor due to the j^{th} source, $s_j(t)$ is the slowly varying envelope of the signal from j^{th} source with variance

$$\sigma_j^2=E[|s_j(t)|^2];\ j=1,...,J. \tag{6}$$

We define the array signal vector as

$$\mathbf{x}(t)=\mathbf{P}\mathbf{s}(t)\in C^{4M\times 1}, \tag{7}$$

where

$$\mathbf{s}(t)=[s_1(t),...,s_J(t)]^T\in C^{J\times 1} \tag{8}$$

is the source signal vector, and $\mathbf{P}$ is the matrix defined as,

$$\mathbf{P}=[\mathbf{p}(\phi_1,r_1,z_1)....\mathbf{p}(\phi_J,r_J,z_J)]\in C^{4M\times J}, \tag{9}$$

where each $\mathbf{p}(\phi_j,r_j,z_j)\in C^{4M\times 1}$ is the array signal amplitude vector defined as

$$\mathbf{p}(\phi_j,r_j,z_j)=[p_{1j}\ \bar{v}_{x1j}\ \bar{v}_{y1j}\ \bar{v}_{z1j}...p_{Mj}\ \bar{v}_{xMj}\ \bar{v}_{yMj}\ \bar{v}_{zMj}]^T, \tag{10}$$

with

$$\bar{v}_{xmj}=\rho c(z)v_{xmj},\ \bar{v}_{ymj}=\rho c(z)v_{ymj},\ \bar{v}_{zmj}=\rho c(z)v_{zmj} \tag{11}$$

for $m=1,...,M$. The particle velocity components are multiplied by $\rho c(z)$ to render the elements of $\mathbf{P}$ dimensionally uniform. The elements of $\mathbf{p}(\phi_j,r_j,z_j)$ can be obtained from (1) - (4). Each vector $\mathbf{p}(\phi_j,r_j,z_j)$ can further be written as

$$\mathbf{p}(\phi_j,r_j,z_j)=\mathbf{A}(\phi_j)\mathbf{b}(r_j,z_j), \tag{12}$$

where

$$\mathbf{b}(r_j,z_j)=\left[b_{1j},...,b_{Nj}\right]^T\in C^{N\times 1};\ j=1,...,J \tag{13}$$

are the mode amplitude vectors with b_{nj} given by (5).

$$\mathbf{A}(\phi_j)=\left[\mathbf{a}(\phi_j,k_1)...\mathbf{a}(\phi_j,k_N)\right]\in C^{4M\times N} \tag{14}$$

is a matrix whose columns are the steering vectors defined as

$$\mathbf{a}(\phi_j,k_n)=\left[\mathbf{a}_1^T(\phi_j,k_n)...\mathbf{a}_M^T(\phi_j,k_n)\right]^T\in C^{4M\times 1},n=1,...,N \tag{15}$$

and

$$\mathbf{a}_m(\phi_j,k_n)=\left[1\ \ \frac{k_n cos\phi_j}{k(z)}\ \ \frac{k_n sin\phi_j}{k(z)}\ \ \frac{-i\psi_n'(z)}{k(z)\psi_n(z)}\right]^T e^{i(m-1)dk_n cos\phi_j}. \tag{16}$$

The function $\psi_n'(z)$ is the derivative of $\psi_n(z)$. The array data vector, including additive noise, can be written as

$$\mathbf{y}(t)=\mathbf{P}\mathbf{s}(t)+\mathbf{n}(t). \tag{17}$$

The array noise vector $\mathbf{n}(t)$ is given by

$$\mathbf{n}(t)=\left[\mathbf{n}_1^T(t)...\mathbf{n}_M^T(t)\right]^T\in C^{4M\times 1}, \tag{18}$$

where

$$\mathbf{n}_m(t)=\left[n_{p,m}(t)\ \rho c(z)n_{vx,m}(t)\ \rho c(z)n_{vy,m}(t)\ \rho c(z)n_{vz,m}(t)\ \right]^T \tag{19}$$

is the 4×1 vector of noise components at the m^{th} sensor.

3. WHITENING TRANSFORMATION

We assume that (i) the elements of the source signal vector $\mathbf{s}(t)$ are mutually uncorrelated, and (ii) the noise vectors $[\mathbf{n}_m(t);\ m=1,...,M]$ are identically distributed, mutually uncorrelated, and also uncorrelated with the signal vector $\mathbf{s}(t)$. However, there exists correlation among the elements of each noise vector $\mathbf{n}_m(t)$. Hence, using (17), the array data covariance matrix can be written as

$$\mathbf{C}_y=E[\mathbf{y}(t)\mathbf{y}^H(t)]=\mathbf{P}\mathbf{C}_s\mathbf{P}^H+\mathbf{C}_n, \tag{20}$$

where

$$\mathbf{C}_s=E[\mathbf{s}(t)\mathbf{s}^H(t)]=diag\left(\sigma_1^2,...,\sigma_J^2\right) \tag{21}$$

is the source signal covariance matrix and

$$\mathbf{C}_n=E[\mathbf{n}(t)\mathbf{n}^H(t)]=\sigma^2 diag\left(\Upsilon,....,\Upsilon\right) \tag{22}$$

is a $4M\times 4M$ block diagonal array noise covariance matrix where Υ is a 4×4 noise covariance matrix at each vector sensor. We assume that noise is predominantly wind-generated noise, for which the covariance matrix can be shown to be [6]

$$\Upsilon(z)=\begin{bmatrix}\xi(z) & & & \zeta(z)\\ & \xi_x(z) & & \\ & & \xi_y(z) & \\ \zeta(z) & & & \xi_z(z)\end{bmatrix}\in C^{4\times 4} \tag{23}$$

where

$$\xi(z)=\sum_{n=1}^{N}\psi_n^2(z), \tag{24}$$

$$\xi_x(z)=\xi_y(z)=\frac{1}{2}\sum_{n=1}^{N}\psi_n^2(z), \tag{25}$$

$$\xi_z(z)=\left(\frac{1}{k(z)}\right)^2\sum_{n=1}^{N}\psi_n'^2(z), \tag{26}$$

$$\zeta(z)=\frac{1}{k(z)}\sum_{n=1}^{N}\psi_n(z)\psi_n'(z). \tag{27}$$

The array noise vector $\mathbf{n}(t)$ can therefore be whitened through the transformation $\mathbf{n}_w(t)=\mathbf{W}\mathbf{n}(t)$ where

$$\mathbf{W}=diag\left(\Upsilon^{-1/2},...,\Upsilon^{-1/2}\right) \tag{28}$$

is a depth-dependent $4M\times 4M$ whitening matrix. The whitened array data vector is given by

$$\mathbf{y}_w(t)=\mathbf{W}\mathbf{P}\mathbf{s}(t)+\mathbf{W}\mathbf{n}(t), \tag{29}$$

and the whitened array data covariance matrix is

$$\mathbf{C}_{yw}=E\left[\mathbf{y}_w(t)\mathbf{y}_w^H(t)\right]=\mathbf{W}\mathbf{P}\mathbf{C}_s\mathbf{P}^H\mathbf{W}^H+\sigma^2\mathbf{I}. \tag{30}$$

4. SUBSPACE INTERSECTION METHOD

In (30), $\mathbf{C}_s$ is a diagonal matrix of rank J, and $\mathbf{W}$ is an invertible square matrix of rank $4M$. It can be shown following an approach similar to that in reference [4] that the J columns of the $4M\times J$ matrix $\mathbf{P}$ are linearly independent for every set of J distinct source positions if $4M\geq NJ$. In the following analysis, we assume that the condition $4M\geq NJ$ is satisfied. It follows that the matrix $\mathbf{W}\mathbf{P}\mathbf{C}_s\mathbf{P}^H\mathbf{W}^H$ is of rank J. The signal subspace $\boldsymbol{S}$ is defined as

$$\boldsymbol{S}=\text{span}\left\{\mathbf{u}_1,...,\mathbf{u}_J\right\}=\text{span}\ \left\{\mathbf{W}\mathbf{p}(\phi_1,r_1,z_1),....,\mathbf{W}\mathbf{p}(\phi_J,r_J,z_J)\right\} \tag{31}$$

where $\mathbf{u}_1,...,\mathbf{u}_J$ are the 'signal' eigenvectors of $\mathbf{C}_{yw}$ corresponding to the J largest eigenvalues. We define the modal subspace $\boldsymbol{M}(\phi)$ for azimuth ϕ as

$$\boldsymbol{M}(\phi) = \text{span}\{\mathbf{Wa}(\phi,k_1),...,\mathbf{Wa}(\phi,k_N)\}, \tag{32}$$

where $\mathbf{a}(\phi,k_n)$ is the modal steering vector defined in (15) and (16). It is evident that $\boldsymbol{M}(\phi) \neq \boldsymbol{M}(\tilde{\phi})$ for $\phi \neq \tilde{\phi}$. It follows from (12) and (32) that $\mathbf{Wp}(\phi_j,r_j,z_j) \in \boldsymbol{M}(\phi_j)$ for $j = 1,...,J$. We also have $\mathbf{Wp}(\phi_j,r_j,z_j) \in \boldsymbol{S}$ for $j = 1,...,J$. It follows that $\boldsymbol{S}$ and $\boldsymbol{M}(\phi)$ intersect if $\phi \in \{\phi_1,\phi_2,...,\phi_J\}$.

Finally, we note that $\boldsymbol{S}$ and $\boldsymbol{M}(\phi)$ intersect only if a nontrivial linear combination of the linearly independent basis vectors of $\boldsymbol{S}$ and $\boldsymbol{M}(\phi)$ is a null vector. Consider a linear combination with $N+J-1$ complex numbers $c_1,...,c_{N+J-1}$ and a real number ϕ such that

$$\sum_{j=1}^{J} c_j \mathbf{p}(\phi_j,r_j,z_j) + \sum_{n=1}^{N-1} c_{J+n}\mathbf{a}(\phi,k_n) + \mathbf{a}(\phi,k_N) = \mathbf{0}. \tag{33}$$

This set comprises $4M$ complex equations with $N+J-1$ complex unknowns $c_1,...,c_{N+J-1}$ and one real unknown. For $4M \geq N+J$, the number of equations exceeds the number of unknowns and a solution for (33) exists only if $\phi \in \{\phi_1,...,\phi_J\}$. It follows that $\boldsymbol{S}$ and $\boldsymbol{M}(\phi)$ intersect if and only if $\phi \in \{\phi_1,...,\phi_J\}$.

We now proceed to perform the bearing estimation of sources in shallow ocean using the acoustic vector sensor array. The procedure is similar to the subspace intersection method for a scalar sensor array. Let us construct a $4M \times (N+J)$ matrix $\mathbf{D}(\phi)$ defined as follows:

$$\mathbf{D}(\phi) = [\alpha_1\mathbf{Wa}(\phi,k_1)....\alpha_N\mathbf{Wa}(\phi,k_N)\ \mathbf{u}_1....\mathbf{u}_J]. \tag{34}$$

where $\alpha_1,...,\alpha_N$ are normalizing constants. Further, the first M columns of $\mathbf{D}(\phi)$ are linearly independent basis vectors of the modal subspace $\boldsymbol{M}(\phi)$ and the remaining J columns are the orthonormal basis vectors of the signal subspace $\boldsymbol{S}$. We then perform a QR decomposition to factorize the matrix $\mathbf{D}(\phi)$ as

$$\mathbf{D}(\phi) = \mathbf{Q}(\phi)\mathbf{R}(\phi). \tag{35}$$

Here,

$$\mathbf{Q}(\phi) = [\mathbf{q}_1(\phi)....\mathbf{q}_{N+J}(\phi)] \tag{36}$$

is an $4M \times (N+J)$ matrix whose columns $\mathbf{q}_i(\phi)$ are orthonormal vectors and $\mathbf{R}(\phi)$ is a $(N+J)\times(N+J)$ upper triangular matrix whose diagonal elements are the eigenvalues of the matrix $\mathbf{D}(\phi)$. The columns of $\mathbf{D}(\phi)$ are related to the columns of $\mathbf{Q}(\phi)$ through the equations

$$\mathbf{d}_i(\phi) = \sum_{k=1}^{i} r_{ki}(\phi)\mathbf{q}_k(\phi),\ i = 1,...,N+J \tag{37}$$

where $\mathbf{d}_i(\phi)$ is the i^{th} column of $\mathbf{D}(\phi)$ and $r_{ki}(\phi)$ is the $(k,i)^{th}$ element of $\mathbf{R}(\phi)$. The elements $r_{ki}(\phi)$ and the vectors $\mathbf{q}_k(\phi)$ can be determined recursively using the relations

$$r_{11}(\phi) = \|\mathbf{d}_1(\phi)\|_2, \tag{38}$$

$$\mathbf{q}_1(\phi) = \frac{1}{r_{11}(\phi)}\mathbf{d}_1(\phi), \tag{39}$$

$$r_{ki}(\phi) = \mathbf{q}_k^H(\phi)\mathbf{d}_i(\phi), 1 \leq k \leq i-1;\ i = 2,...,(N+J) \tag{40}$$

$$r_{ii}(\phi) = \left\| \mathbf{d}_i(\phi) - \sum_{k=1}^{i-1} r_{ki}(\phi)\mathbf{q}_k(\phi) \right\|_2;\ i = 2,...,(N+J) \tag{41}$$

$$\mathbf{q}_i(\phi) = \frac{\mathbf{d}_i(\phi) - \sum_{k=1}^{i-1} r_{ki}(\phi)\mathbf{q}_k(\phi)}{r_{ii}(\phi)};\ i = 2,...,(N+J) \tag{42}$$

where $\|\ .\ \|_2$ denotes the Euclidean norm. A diagonal element $r_{ii}(\phi)$ of the matrix $\mathbf{R}(\phi)$ is zero if and only if $\mathbf{d}_i(\phi) \in \text{span}\{\mathbf{d}_1(\phi),...,\mathbf{d}_{i-1}(\phi)\}$. This property will be exploited during the formulation of the bearing estimation algorithm.

Assuming that $4M \geq NJ$ and $4M \geq (N+J)$, we know that the subspaces $\boldsymbol{M}(\phi) = \text{span}\{\mathbf{d}_1(\phi),...,\mathbf{d}_N(\phi)\}$ and $\boldsymbol{S} = \text{span}\{\mathbf{d}_{N+1},...,\mathbf{d}_{N+J}\}$ intersect if and only if $\phi \in \{\phi_1,\phi_2,...,\phi_J\}$. Therefore, it follows that $\phi \in \{\phi_1,\phi_2,...,\phi_J\}$ if and only if one of the following conditions is satisfied:

$$\mathbf{d}_i \in \text{span}\{\mathbf{d}_1(\phi),...,\mathbf{d}_N(\phi)\};\ i \in \{N+1,...,N+J\} \tag{43}$$

$$\text{or } \mathbf{d}_{N+J} \in \text{span}\{\mathbf{d}_1(\phi),...,\mathbf{d}_{N+J-1}(\phi)\} \tag{44}$$

Thus, we have the following result: $\mathbf{d}_i \in \text{span}\{\mathbf{d}_1(\phi),...,\mathbf{d}_{i-1}(\phi)\}$ for some $i \in \{N+1,...,N+J\}$ if and only if $\phi \in \{\phi_1,...,\phi_J\}$.

Since $r_{ii}(\phi) = 0$ if and only if $\mathbf{d}_i(\phi) \in \text{span}\{\mathbf{d}_1(\phi),...,\mathbf{d}_{i-1}(\phi)\}$, it follows that $r_{ii}(\phi) = 0$ for some $i \in \{(N+1),...,(N+J)\}$ if and only if $\phi \in \{\phi_1,...,\phi_J\}$. Hence, the SIM response function

$$B_{SI}(\phi) = \left[\min_{N+1 \leq i \leq N+J} | r_{ii}(\phi) | \right]^{-1} \tag{45}$$

has sharp peaks at $\phi = \phi_1,\phi_2,...,\phi_J$.

5. RESULTS AND DISCUSSION

We consider a Pekeris model of the ocean [7], so that $c(z)$, $c_b(z)$, $\rho(z)$ and $\rho_b(z)$ are independent of z. All simulations have been performed with the following values of channel parameters: $c = 1500$ m/s, $c_b = 1700$ m/s, $\rho_b/\rho = 1.5$, and attenuation in the ocean bottom is $\delta = 0.5$ dB/λ, where λ is the free space wavelength. An array of vector sensors is assumed to be at a depth $z = 25$ m below the surface of the ocean. The ocean depth h is 100 m and the source signal frequency f is 50Hz. For this choice of parameters, the number of modes is $N = 6$. Independent samples of uniformly distributed random phases were added to the signal from each source to render the sources noncoherent. Independent samples of a zero-mean complex Gaussian random vector with covariance matrix $\sigma^2\text{diag}(\Upsilon...\Upsilon)$ were used to generate the noise vector $\mathbf{n}(t)$. The parameter σ^2 was adjusted to yield the desired signal-to-noise ratio (SNR), defined as

$$SNR = 10\log_{10}\frac{\sum_{m=1}^{M}\sum_{j=1}^{J}\sigma_j^2 \mid \mathbf{p}_{mj} \mid^2}{M\sigma^2\xi}, \tag{46}$$

where σ_j^2 is the source power given by (6), ξ is defined in (24), and $\sigma^2\xi$ is the variance of pressure component of noise.

The covariance matrix $\mathbf{C}_{yw}$ was estimated from the whitened data vector $\mathbf{y}_w(t)$ by averaging $\mathbf{y}_w(t)\mathbf{y}_w^H(t)$ over L snapshots

$$\hat{\mathbf{C}}_{yw} = \frac{1}{L}\sum_{t=1}^{L}\mathbf{y}_w(t)\mathbf{y}_w^H(t). \tag{47}$$

Eigenvectors of $\hat{\mathbf{C}}_{yw}$ corresponding to the J largest eigenvalues provide estimates of the signal eigenvectors $\mathbf{u}_1,...,\mathbf{u}_J$. Simulations have been performed by considering data obtained using both conventional scalar sensors and vector sensors to localize the sources. The sources are located at equal ranges $r_j = 5000$ m and equal depths $z_j = 37.5$ m. The spacing between sensor elements is $d = \lambda/2 = 15$ m, unless otherwise stated. The number of snapshots is $L = 350$ unless otherwise stated. All results have been generated by averaging over 250 simulations.

A comparative performance analysis of SIM with AVS and scalar sensor arrays is presented in Figs.1-10. A typical SIM

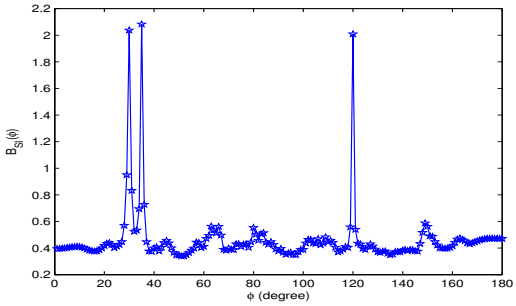

Figure 1: SIM ambiguity function for AVS array with M=10, SNR=20dB. Three sources are at $30^0, 35^0, 120^0$.

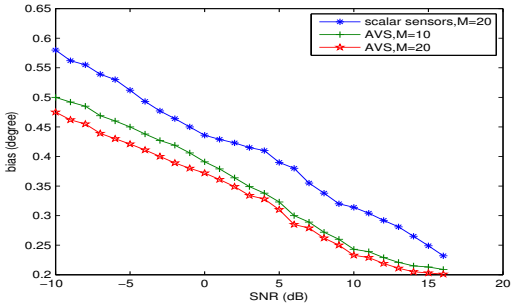

Figure 2: Variation of bias with SNR for AVS array with M=10,20 and scalar sensor array with M=20. The source is at 60^0.

response function $B_{SI}(\phi)$ is shown in Fig.1, which corresponds to a 10-sensor AVS array when the source bearing angles are 30^0, 35^0 and 120^0. Figures 2 and 3 show respectively the plots of bias and root mean square error (RMSE) versus SNR. The Cramer-Rao bound (CRB) for a 20-sensor AVS array is also shown in Fig.3. It is seen that (i) the AVS array performs significantly better than a scalar sensor array, and (ii) the RMSE of SIM for the AVS array is quite close to the CRB. Similar conclusions can be drawn from Fig.4 which shows the variation of RMSE with the number of sensors M. The bias and rms error seen in Figs.2-4 are due to the error in estimation of the covariance matrix $\mathbf{C}_{yw}$ using a finite number of snapshots L. Figures 5 and 6 indicate that both bias and RMSE approach zero asymptotically with increasing L. Figure 7 shows the plots of RMSE versus the bearing angle ϕ for both AVS and scalar sensor array and the plot of CRB versus ϕ for the AVS array. For the scalar sensor array, the dimension of the $N-$dimensional modal subspace $\boldsymbol{M}(\phi)$ collapses to unity at $\phi = 90^0$. Hence, the RMSE of SIM for the scalar sensor array rises rapidly as ϕ approaches 90^0 (broadside direction). Since the dimension of $\boldsymbol{M}(\phi)$ for the AVS array is N for all ϕ including $\phi = 90^0$, the RMSE of SIM for the AVS array remains low in the vicinity of broadside. For both arrays RMSE is high near the endfire direction ($\phi = 0^0$). Figure 8 shows the plot of probability of detection of two closely spaced sources versus the angular separation $\delta\phi$ for the AVS and scalar sensor arrays, illustrating the superior resolving capability of the AVS array.

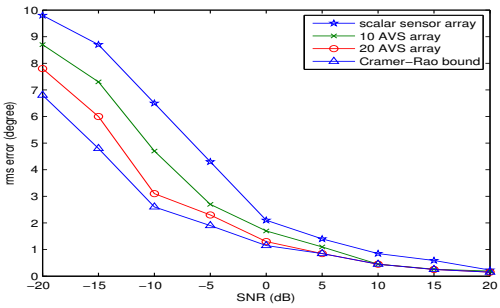

Figure 3: Variation of RMSE with SNR for AVS array with M=10,20 and scalar sensor array with M=20. CRB for AVS array with M=20 is also shown. Source is at 60^0.

For unambiguous bearing estimation, the steering vectors have to satisfy the condition

$$\mathbf{a}(\phi, k_n) = \mathbf{a}(\phi', k_{n'}) \text{ only if } \phi = \phi',\ n = n'. \tag{48}$$

For a scalar sensor array, the vector

$$\mathbf{a}(\phi, k_n) = \left[1\ e^{idk_n cos\phi} \ldots e^{i(M-1)dk_n cos\phi}\right]^T$$

may not satisfy condition (48) if $d > \pi/k_1 = \lambda_1/2$. For an AVS array, $\mathbf{a}(\phi, k_n) \in C^{4M\times 1}$ has a more complex structure as seen from (15) and (16), and hence condition (48) is always satisfied even if $d > \lambda_1/2$. The absence of any constraint on the intersensor spacing d can be exploited to enhance the resolution of an AVS array by choosing a larger value of d. Figures 9 and 10 show the SIM response function for AVS array and scalar sensor array respectively for $d = 3\lambda \simeq 3\lambda_1$, when two sources are located at 80^0 and 82^0. The AVS array resolves the two sources and estimates their bearing angles unambiguously. For a scalar sensor array, unambiguous estimation is not possible due to the presence of a large number of sidelobes.

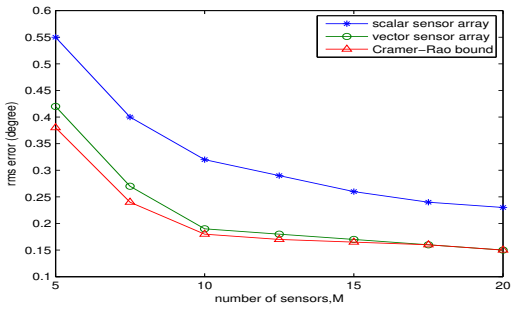

Figure 4: Variation of RMSE with M for AVS and scalar sensor arrays. CRB for AVS array is also shown. SNR=20dB. Source is at 60^0.

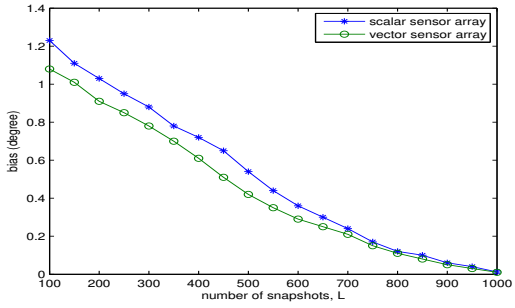

Figure 5: Variation of bias with the number of snapshots for scalar and AVS arrays. M=10, SNR=10dB. Source is at 60^0.

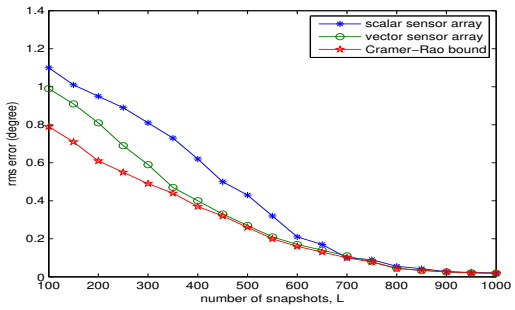

Figure 6: Variation of RMSE with the number of snapshots for scalar and AVS arrays. CRB for AVS array is also shown. M=10, SNR=10dB. Source is at 60^0.

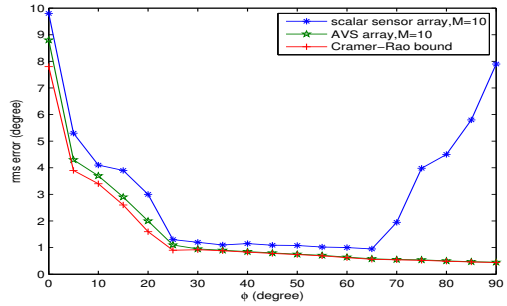

Figure 7: Variation of RMSE with the bearing angle for AVS and scalar sensor arrays. CRB for AVS array is also shown. M=10, SNR=20 dB

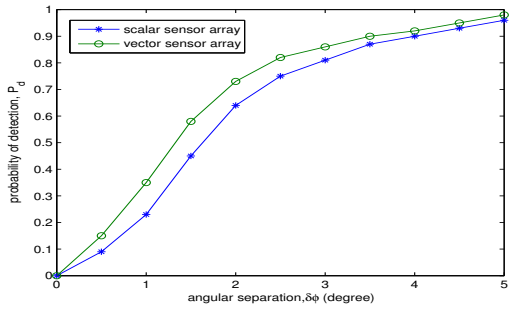

Figure 8: Probability of detection versus angular separation between 2 sources. Source 1: 60^0. Source 2: $60^0 + \delta\phi$. M=10, SNR=20dB.

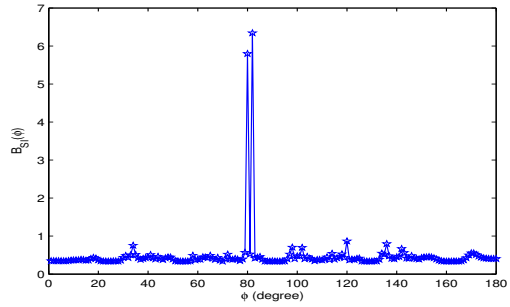

Figure 9: SIM Response function of AVS array with $d = 3\lambda$ for 2 sources at 80^0 and 82^0. M=20, SNR=20dB.

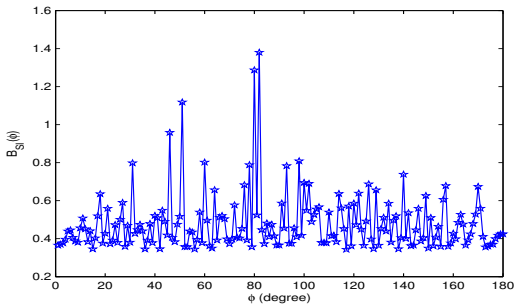

Figure 10: SIM Response function of scalar sensor array for the same conditions as in Fig. 9.

6. CONCLUSIONS

In this paper, we have presented the subspace intersection method (SIM) of high-resolution bearing estimation in a range-independent shallow ocean using a horizontal linear array of acoustic vector sensors (AVS). The bearing angles are estimated using a one-dimensional search algorithm which does not assume prior knowledge of source ranges and depths. The minimum number of sensors required by the SIM algorithm reduces by a factor of 4 if scalar sensors are replaced by vector sensors; the requirement is $M \geq NJ$ for scalar sensors and $M \geq \frac{1}{4}NJ$ for vector sensors. For an AVS array there is no constraint on interelement spacing d, while for a scalar sensor array d cannot exceed $\lambda_1/2$. Hence, with an AVS array, resolution can be enhanced by increasing the spacing d. The performance of SIM with a scalar sensor array degrades drastically for sources near the broadside direction, but SIM with AVS array does not suffer from this drawback. Simulation results show that the bias and rms error for an AVS array are significantly lower than those for a scalar sensor array, especially at low SNR. The AVS array also provides greater resolution than the scalar sensor array.

ACKNOWLEDGMENT

This work was partially supported by the DRDO-IISc Programme of Advanced Research in Mathematical Engineering.

REFERENCES

[1] R.O. Schmidt, "Multiple emitter location and signal parameter estimation", Proceedings of RADC Spectrum Estimation Workshop, Rome Air Development Center, Rome, 1979, pp. 243 - 258.

[2] R. Roy, A. Paulraj, T. Kailath, "ESPRIT - A subspace rotation approach to estimation of paramter of cisoids in noise", *IEEE Trans. Acoust. Speech Signal Process*, vol. 34, pp. 1340 - 1342, 1986.

[3] A. Tolstoy, *Matched Field Processing for Underwater Acoustics*, World Scientific, Singapore, 1993.

[4] S. Lakshmipathi and G.V.Anand, "Subspace intersection method of high-resolution bearing estimation in shallow ocean", *Signal Processing*, vol. 84, pp. 1367-1384, 2004.

[5] A. Nehorai and E. Paldi, "Acoustic vector-sensor array procesing", *IEEE Trans. on Signal Processing*, vol. 42, no. 9, pp. 2481-2491, Sept. 1994.

[6] K.P. Arunkumar, *3- Dimensional Localisation of Acoustic Sources Using Vector Sensors*, M.E. Project Report, Department of Electrical Engineering, Indian Institute of Science, Bangalore, 2007.

[7] L.M. Brekhovskikh, Yu. Lysanov, *Fundamentals of Ocean Acoustics*, Springer, Berlin, 1982 (Chapter 5).